Resonant Damping of Flexible Structures Under Random Excitation

Steen Krenk and Jan Høgsberg

Abstract Structural vibrations are often dominated by resonant response, and increased efficiency in the damping of these vibrations can often be attained by using the resonant properties of these modes. A typical example is the 'tuned mass absorber'. While the original design procedure was based on properties of the frequency response graph, it has recently been demonstrated that the problem can be generalized and solved by use of the complex root-locus properties. The basic principle in this formulation is the introduction of a resonant force with frequency tuning that results in splitting the original resonant mode into two modes with equal damping ratio. Here the basic principle of resonant absorbers is presented in concise form and generalized in two ways. First the principle of resonant absorbers is presented in a general form in terms of sensors and actuators, recording the motion and imposing appropriate forces, respectively. A general design procedure is developed for resonant displacement and acceleration feedback, respectively, based on a combination of 'equal modal damping' and approximately equal response amplitudes of the two modes. This leads to explicit design formulae for the parameters of the control system. The optimal calibration leads to a plateau of near-equal amplification in a frequency interval around the original natural frequency. In multi-degree-of-freedom structures the sensor picks up the total deformation from all the modes that are active at the location of the sensor, and the actuator force acts on all these modes. A quasi-static correction is developed that identifies the part of the sensor signal associated with the mode to be damped and the reduced effect of the actuator on this mode. This correction takes the form of explicit modifications of the formulae for the optimal control parameters, while retaining the original format. The efficiency of resonant damping is illustrated by application to a benchmark example for stochastic wind load on a high-rise building. It is demonstrated that the present resonant damping technique based on a single collocated sensor is competitive with more heavily instrumented configurations using the classic LQG technique.

S. Krenk (✉) and J. Høgsberg
Department of Mechanical Engineering, Technical University of Denmark,
Nils Koppels Allé, Building 403, DK-2800 Kgs. Lyngby, Denmark
e-mail: sk@mek.dtu.dk; jhg@mek.dtu.dk

M. Papadrakakis et al. (eds.), *Computational Methods in Stochastic Dynamics*,
Computational Methods in Applied Sciences 22, DOI 10.1007/978-90-481-9987-7_2,

1 Introduction

There are many situations within structural dynamics, in which there is a need for limiting undesirable oscillations at one or more resonance frequencies, e.g. earthquake response, bridge vibrations, space structures and instruments. In the structural dynamics community this has typically been dealt with by using the concepts from the tuned mass absorber, described e.g. by Den Hartog [1]. The idea is to mount an additional mass with suitable stiffness and damping to introduce a resonant relative motion and to optimize the damping of this relative motion. The traditional design procedure is based on the frequency response curve of an idealized single degree of freedom structure. First the frequency is tuned to balance the magnitude of the resonances of the two modes generated by the combined motion of the idealized structure and the suspended mass, and then the damping is chosen to provide suitable extraction of energy without eliminating the relative motion.

Within the area of structural control the effect is typically obtained by actuators that are controlled by applying a suitable algorithm to signals obtained from sensors on the structure. In this setting the resonant control is typically obtained by a suitable filter that introduces an additional resonance, represented by an additional pole in the complex frequency plane. Common design procedures are based on placement of the complex poles to obtain maximum modal damping, and the intensity of the actuator force is controlled via a gain parameter [2]. In the case of resonant control identification of a suitable format containing a gain parameter is a central part of the design problem.

A common characteristic of most of the work on resonant control from a control theory perspective is its focus of the location of the poles in the complex plane. However, optimal response characteristics also require optimal coupling between control and structure, and may also involve the load – properties that do not show up directly in the root locus diagram. In a recent analysis by Krenk [3] the original response curve design format of the tuned mass damper was recast into root locus format, and it was demonstrated that a key to the efficiency of the classic design procedure is that the two modes generated by interference have identical modal damping ratio. This turns out to be a convenient starting point for the design of resonant dampers. The first step is to select the resonant frequency of the device to produce the 'equal modal damping split'. The remaining parameters should then be chosen to provide a level plateau with suitable damping. This in turn implies that the two involved resonance frequencies are not too closely spaced, as this would produce undesirable constructive interference. This was demonstrated for the tuned mass absorber in [3] and extended to a more general format for resonant damping in terms of sensors and actuators in [4].

In the case of a flexible structure the motion monitored by the sensor will contain components that are not associated with the mode to be controlled. This problem has been addressed in connection with a tuned mass absorber on a multi-degree-of-freedom structure by Ozer and Royston [5,6], who included the additional degree of freedom by use of the Sherman-Morrison formula and established an analogy with the single degree of freedom system and the design procedure of Den Hartog. In its

general form the procedure is rather cumbersome, involving an iteration process. In this paper a simple explicit correction is developed for control of the low-frequency modes. The effect of the higher frequency modes is taken into account by including the corresponding quasi-static terms in the two equations for the simple control problem. The procedure and its efficiency are demonstrated by application to a high-rise building under wind load.

2 Resonant Response Format

The control problem is illustrated in Fig. 1. The structure is represented by a mass m with displacement $x(t)$. The external load on the structure is represented by the force $F(t)$. The control is accomplished via a sensor signal $y(t)$ used to control an additional force $F_c(t)$. Figure 1a illustrates the case of a flexible structure, with the first mode being represented by the mode shape vector $\mathbf{u}_1$ and the modal amplitude x_1. A single-degree-of-freedom representation is obtained, if this mode is considered without including interaction with higher modes. This case will be considered first in Sects. 3 and 4. In some situations it is important to account for the fact that the modal response $\mathbf{u}_1 x_1(t)$ only constitutes part of the total motion. In this case improved damping properties may be obtained by correcting for the contributions from higher frequency modes as discussed in Sect. 5.

The analysis and design of the system will be carried out in the frequency domain. For this purpose the time dependence is represented via the complex exponential function $\exp(i\omega t)$, where ω is the angular frequency, that will typically be complex valued, corresponding to attenuated response. The controller force F_c is obtained from the control variable y, which in turn is obtained by filtering the response x. This can be expressed in the general frequency format

$$\begin{aligned} G_{xx}(\omega)\, x \;+\; G_{xy}(\omega)\, y \;&=\; F/m, \\ G_{yx}(\omega)\, x \;+\; G_{yy}(\omega)\, y \;&=\; 0, \end{aligned} \tag{1}$$

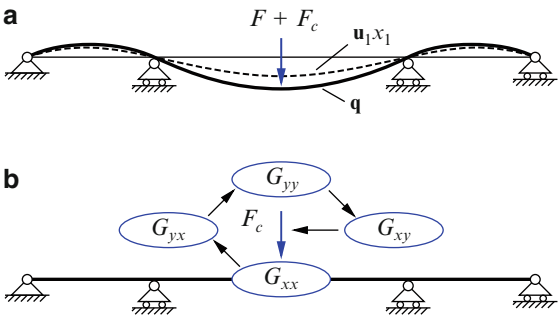

Fig. 1 Structure with sensor and control force: (**a**) Flexible MDOF structure and (**b**) control loop

where F is the external force, and m is the structural mass. $G_{xx}, G_{xy}, \ldots$ are frequency dependent transfer functions, illustrated in Fig. 1b.

The quality of the control is associated with its ability to limit the response of the structure around the resonance frequency ω_s. The response x follows from elimination of the control variable y between the equations in (1), whereby

$$x \;=\; \frac{G_{yy}}{G_{xx}G_{yy} - G_{xy}G_{yx}}\,\frac{F}{m}. \tag{2}$$

Clearly, the magnitude of the control force F_c needed to reduce the resonant response is also of importance. It follows from (1) in the form

$$F_c \;=\; -m\,G_{xy}\,y \;=\; \frac{G_{xy}G_{yx}}{G_{xx}G_{yy} - G_{xy}G_{yx}}\,F. \tag{3}$$

It is seen that the frequency functions G_{xy} and G_{yx} only influence the response x and the control force F_c through the product $G_{xy}G_{yx}$. Interchange of G_{xy} with G_{yx} may lead to a redefinition of the control variable y, but leaves the structural response x and the control force F_c unchanged.

2.1 Structure and Resonator Representation

For a structure without internal damping the natural angular frequency ω_s is given in terms of the stiffness k and mass m as

$$\omega_s^2 = k/m. \tag{4}$$

Thus, the free response of the structure is governed by the frequency function

$$G_{xx}(\omega) \;=\; \omega_s^2 - \omega^2. \tag{5}$$

In this formulation the effect of structural damping has been omitted because it is usually small for structures needing additional damping devices and furthermore it complicates the analysis considerably. A simple combination format for structural and controller induced damping has been obtained in [7] for the tuned mass absorber, corresponding to the case of acceleration feedback in the present context.

The controller consists of an oscillator defined by the second order filter function

$$G_{yy}(\omega) \;=\; \omega_c^2 - \omega^2 + 2i\,\zeta_c\omega_c\omega, \tag{6}$$

where ω_c represents a characteristic angular frequency, and the non-dimensional parameter ζ_c defines the bandwidth of the filter. In the case of a tuned mass vibration absorber ω_c and ζ_c are simply the undamped natural frequency and the damping ratio of the suspended mass system if connected to a rigid support [1, 3].

2.2 Feedback Filters

It is desirable that the control force ratio F_c/F vanishes at zero and infinite frequencies. Within the present format this implies that the product $G_{xy}G_{yx}$ can contain cubic, quadratic and linear terms, but neither a constant or a quartic term. This condition is satisfied by generalized acceleration and displacement feedback. In the following these two feedback forms are treated separately, using general expressions containing the terms from both formulations.

In the generalized acceleration feedback format the motion is monitored via the acceleration, e.g. by an accelerometer, corresponding to the feedback function

$$G_{yx}(\omega) \;=\; \omega^2. \tag{7}$$

The product $G_{xy}G_{yx}$ is limited to a cubic polynomial. The actuator is controlled by a feedback function with an imaginary part to enable tuning of the phase,

$$G_{xy}(\omega) \;=\; \alpha\,\omega_c^2 + \beta\,2i\,\zeta_c\omega_c\omega, \tag{8}$$

with gain parameters α and β. The design problem consists in the determination of optimal combinations of the frequency ratio ω_c/ω_s, the bandwidth parameter ζ_c, and the two gain parameters α and β.

In the case of displacement feedback the displacement is sampled directly, corresponding to a constant frequency function

$$G_{yx}(\omega) \;=\; \omega_c^2, \tag{9}$$

where the frequency ω_c from the resonant controller has been used for dimensional reasons. The actuator frequency function G_{xy} combines a quadratic and a linear term in ω in order to enable tuning of the phase,

$$G_{xy}(\omega) \;=\; \alpha\,\omega^2 + \gamma\,2i\,\zeta_c\omega_s\omega. \tag{10}$$

Here the structure reference frequency ω_s has been used, and two non-dimensional gain factors α and γ have been introduced.

These cases of acceleration feedback and displacement feedback can be combined via the product formula

$$G_{xy}(\omega)G_{yx}(\omega) \;=\; \alpha\,\omega_c^2\omega^2 + 2i\,\zeta_c\omega_c\omega\big(\beta\,\omega^2 + \gamma\,\omega_c\omega_s\big), \tag{11}$$

which covers both cases by setting $\gamma = 0$ and $\beta = 0$, respectively. The denominator then follows from combining the response functions G_{xx} and G_{yy} from (5) and (6) with this expression:

$$\begin{aligned} G_{xx}G_{yy} - G_{xy}G_{yx} = \omega^4 - \left[\omega_s^2 + (1+\alpha)\omega_c^2\right]\omega^2 + \omega_s^2\omega_c^2 \\ - 2i\,\zeta_c\omega_c\omega\left[(1+\beta)\omega^2 - \omega_s^2 + \gamma\omega_s\omega_c\right]. \end{aligned} \tag{12}$$

The roots of this quartic polynomial determine the complex resonance frequencies, and thereby the damping properties of the resonant modes.

3 Root Locus Diagram

The following root locus analysis generalizes that of the tuned mass absorber presented in [3]. Let the four roots of the characteristic equation be denoted $\omega_1, \ldots, \omega_4$, and assume that there is a parameter combination for which ω_1 and ω_2 lie in the first quadrant. The corresponding modes will then have equal damping ratio, if ω_1 and ω_2 lie on the same line containing the origin of the complex plane as illustrated in Fig. 2. This implies that they are inverse points in the complex plane with respect to some real-valued frequency ω_0, i.e.

$$\frac{\omega_2}{\omega_0} = \frac{\omega_0}{\omega_1^*}, \tag{13}$$

where ω_1^* denotes the conjugate of ω_1. The reciprocal relation between ω/ω_0 and ω_0/ω suggests the following format of the characteristic equation,

$$\left(\frac{\omega}{\omega_0} - \frac{\omega_0}{\omega}\right)^2 - 4i\lambda\,\xi\left(\frac{\omega}{\omega_0} - \frac{\omega_0}{\omega}\right) - 4\xi^2 = 0. \tag{14}$$

This equation contains two coefficients, and it turns out to be convenient to express these in terms of the real-valued parameters ξ and λ as shown. The corresponding polynomial form follows from multiplication with $(\omega_0\omega)^2$,

$$\omega^4 - (2 + 4\xi^2)\,\omega_0^2\omega^2 + \omega_0^4 - 4i\lambda\,\xi\omega_0\omega\big(\omega^2 - \omega_0^2\big) = 0. \tag{15}$$

It is seen that the reference frequency ω_0 is defined by the constant term of the normalized characteristic polynomial. The special property of equally damped modes as expressed by the inverse root relation (13) is equivalent to imposing a balance between the cubic and linear terms, whereby they cancel at the frequency $\omega = \pm\omega_0$.

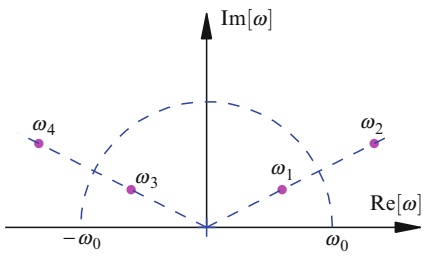

Fig. 2 Complex roots ω_1, ω_2 and ω_3, ω_4 as inverse points of the circle $|\omega| = \omega_0$

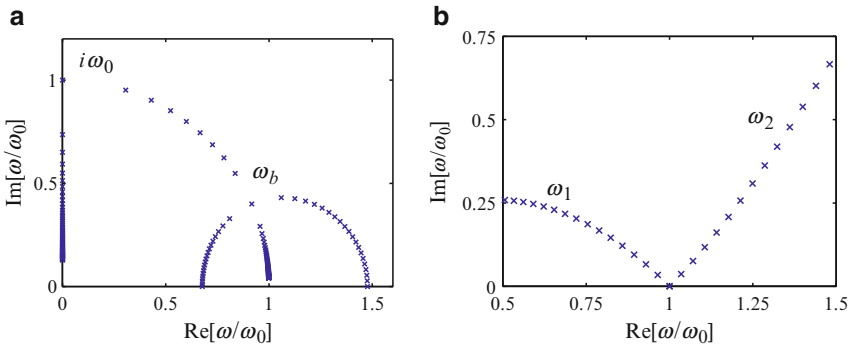

Fig. 3 Root locus diagram: (**a**) $\xi = 0.4$, $\lambda = 0, 0.05, 0.10, \ldots$; (**b**) $\xi = 0, 0.05, 0.10, \ldots$, $\lambda = \frac{1}{2}\sqrt{2}$

The root locus diagram of the quartic equation (15) is easily analyzed by reverting to the quadratic format (14). This format permits determination of the expression inside the parenthesis, and ω then follows from solving a quadratic equation, see e.g. [3, 4] for details. The results are illustrated in Fig. 3. For $\lambda = 0$ there is no damping, and the natural frequencies ω_1 and ω_2 appear as points on the positive real axis. When increasing λ for a fixed value of the parameter $\xi < 1$, the roots move into the complex plane as illustrated in Fig. 3a. It follows from the inverse point property, illustrated in Fig. 2, that the two roots ω_1 and ω_2 have equal argument, corresponding to equal damping of the corresponding free modes. This situation changes at the bifurcation point ω_b, which is reached for $\lambda = 1$. The roots then branch off along a circle with radius $|\omega| = \omega_0$. One branch reaches a branch point on the imaginary axis and the other follows the circle towards the real axis.

The parameter values of interest in connection with control and damping of structures correspond to the first part where the roots are inverse points in the circle, i.e. the parameter interval $0 < \lambda \leq 1$. In this parameter interval the two complex roots have the form

$$\omega_{1,2} = |\omega_{1,2}|\big(\sqrt{1-\zeta^2} + i\zeta\big), \tag{16}$$

where ζ is the common damping ratio of the two modes. A simple expression for the modal damping ratio ζ in terms of the system parameters λ and ξ can be obtained by using the fact that the coefficient of the cubic term in (15) is the sum of the four roots $\omega_1, \ldots, \omega_4$. When using the special properties of the four roots illustrated in Fig. 2, the following expression is obtained for the damping ratio

$$\zeta = \frac{\lambda\,\xi}{\frac{1}{2}\Big(\frac{|\omega_1|}{\omega_0} + \frac{\omega_0}{|\omega_1|}\Big)} \simeq \lambda\,\xi, \tag{17}$$

where the latter approximation is valid for small values of ξ, typical of practice.

It may appear desirable to choose λ corresponding to the bifurcation point, as this introduces maximum damping in the modes. However, this also implies identical

angular frequency of the modes and thereby leads to constructive interference of the two modes. As it turns out, an optimal balance between the obtained damping and a suitable separation of the vibration frequencies leads to the parameter value $\lambda = \frac{1}{2}\sqrt{2}$. The local part of the corresponding root locus diagram is illustrated in Fig. 3b. The two roots ω_1 and ω_2 move into the complex plane along curves forming an angle of $\pm 45°$ with the real axis, leading to a modal damping ratio of

$$\zeta \simeq \tfrac{1}{2}\sqrt{2}\,\xi. \tag{18}$$

The following task is to express the optimal properties in terms of the filter parameters and to optimize the corresponding response amplitudes.

4 Optimal Parameters

The root locus analysis of the previous section has identified a characteristic angular frequency ω_0 and determined a condition for equal modal damping in terms of ω_0. The characteristic frequency is determined from the constant term in the polynomial (12),

$$\omega_0^2 = \omega_s\,\omega_c. \tag{19}$$

The condition of equal modal damping consists of the vanishing of the imaginary part of the denominator (12), when evaluated at the reference frequency $\omega = \omega_0$. This gives the equation

$$\omega_s^2 - \gamma\,\omega_s\omega_c = (1+\beta)\omega_0^2. \tag{20}$$

Substitution of the reference frequency ω_0 from (19) then gives the controller frequency as

$$\omega_c = \frac{\omega_s}{1+\beta+\gamma} \tag{21}$$

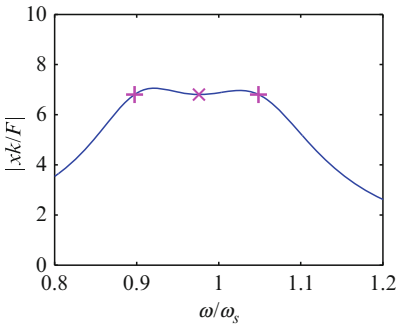

Fig. 4 Equal displacement amplification at three frequencies

Table 1 Optimal parameters for resonant damping in terms of β or γ

Parameter	Acceleration feedback	Displacement feedback
ω_c	$\omega_s/(1+\beta)$	$\omega_s/(1+\gamma)$
ω_0^2	$\omega_c\omega_s$	$\omega_c\omega_s$
α	β	$\gamma(1-\gamma)$
ζ_c^2	$\frac{1}{2}\frac{\beta}{1+\beta}$	$\frac{\gamma}{4}\frac{2+\gamma}{1+\gamma}$

and the reference frequency by

$$\omega_0^2 = \frac{\omega_s^2}{1+\beta+\gamma}. \tag{22}$$

These expressions are included in Table 1, containing the full set of optimal parameters for the two cases.

The principle for determination of the optimal value of the remaining two parameters α and ζ_c is quite simple, although the computations are a bit elaborate. Both parameters are determined from properties of the frequency response (2). An optimal response curve is illustrated in Fig. 4. It turns out that for both the cases under consideration the frequency response curve for $|xk/F|$ has two points at frequencies ω_A and ω_B, marked by the symbol $+$, where the amplitude is independent of the control damping ratio parameter ζ_c. The parameter α is determined by the condition that the amplitude $x(\omega)k/F$ at the two frequencies ω_A and ω_B are equal. This determines the parameter α as

$$\alpha = \beta\,, \quad \gamma = 0 \tag{23}$$

in the case of acceleration feedback, and

$$\alpha = \gamma\,(1-\gamma)\,, \quad \beta = 0 \tag{24}$$

in the case of displacement feedback. This principle has been used by Den Hartog [1] to determine the frequency ratio of a tuned mass absorber, which is a special case of acceleration feedback. In [3] it was demonstrated that for the tuned mass absorber, this criterion is equivalent to the equal modal damping criterion discussed in Sect. 3. In the general case(s) considered here, the equal modal damping criterion determines the frequency ω_c of the controller, while the equal amplification criterion then determines the gain parameter α.

The idea of a resonance damper is that the amplitude should be limited around the resonance frequencies. A particularly simple and robust way of obtaining near-uniform amplification in an interval around the resonance frequencies is to require the amplification at the reference frequency ω_0, marked by the symbol $\times$ in Fig. 4, to be equal to that at ω_A and ω_B, [3]. This condition is used to determine the remaining

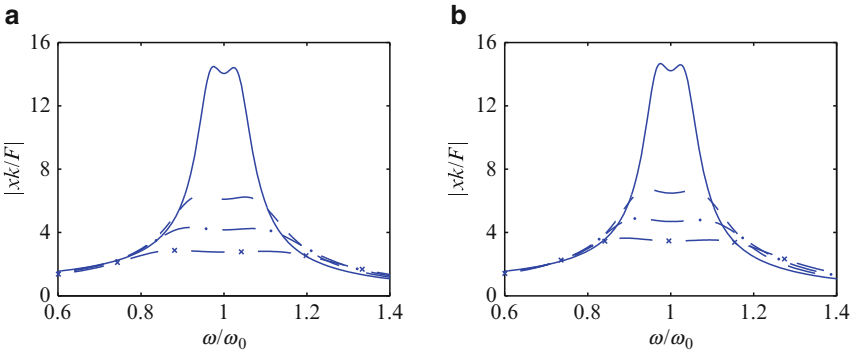

Fig. 5 Frequency response amplitude: $\beta, \gamma = 0.01$ (——), 0.05 (– – –), 0.1 (– · –) and 0.2 (– × –). (**a**) Acceleration feedback, (**b**) displacement feedback

parameter ζ_c. For acceleration feedback this leads to

$$\zeta_c^2 = \frac{1}{2}\frac{\beta}{1+\beta}, \qquad \gamma = 0 \tag{25}$$

while displacement feedback gives

$$\zeta_c^2 = \frac{\gamma}{4}\frac{2+\gamma}{1+\gamma}, \qquad \beta = 0. \tag{26}$$

These optimal parameters are included in Table 1.

The response characteristics of the two types of devices are illustrated in Fig. 5. They are quite similar with maximum values

$$\left|\frac{x\,k}{F}\right|_{\omega_0} \simeq \sqrt{2/\beta} \qquad \text{and} \qquad \left|\frac{x\,k}{F}\right|_{\omega_0} \simeq \sqrt{2/\gamma} \tag{27}$$

for the two cases.

The present parameter calibration has the interesting property that each of the equally damped modes have approximately half of the damping ratio ζ_c introduced in the controller. This follows from the generic result (17), when applied to the present calibrated filter combination,

$$\zeta \simeq \tfrac{1}{2}\zeta_c \frac{\omega_c}{\omega_0} \simeq \tfrac{1}{2}\zeta_c. \tag{28}$$

This approximate result, initially derived for the tuned mass damper in [3], is very accurate for realistic damping ratio values. It serves as a convenient starting point in designing an appropriate resonant filter, when a desired modal damping ratio ζ is prescribed.

5 Multi-Degree-of-Freedom Systems

Results for single-degree-of-freedom systems can often be calibrated so that they are representative for modal behavior in multi-degree-of-freedom systems. The typical problem is that the individual mode only accounts for part of the motion registered by a control sensor, and similarly the actuator force excites other modes as well, as illustrated in Fig. 1a. This is the so-called 'spillover' problem. A formulation of truncated modal analysis in which the motion represented by a small number of selected modes is supplemented by a quasi-static representation of the remaining modes goes back to the seventies, see e.g. [8]. In the following a quasi-static correction procedure is developed for resonant control.

5.1 Background Mode Correction in MDOF Systems

Let a multi-degree-of-freedom system be represented by the stiffness matrix $\mathbf{K}$ and the mass matrix $\mathbf{M}$. The displacements are denoted $\mathbf{q}$ and the corresponding external loads $\mathbf{F}$. In addition to the external load an actuator with control signal η is connected to the structure as described by the connectivity vector $\mathbf{w}$. The connectivity vector $\mathbf{w}$ contains the number 1 at the appropriate degree-of-freedom, if it is connected to the surroundings, and a set of numbers 1 and -1 for two degrees-of-freedom that are connected by an actuator. The corresponding frequency equation is

$$(\mathbf{K} - \omega^2\mathbf{M})\,\mathbf{q} = \mathbf{F} - \mathbf{w}\,G_{q\eta}(\omega)\,\eta. \tag{29}$$

The actuator is assumed to be controlled by a collocated signal, i.e. a signal generated by a sensor attached to the same degrees-of-freedom as the actuator. Thus, the actuator signal η is controlled by the frequency equation

$$G_{\eta\eta}(\omega)\,\eta = -G_{\eta q}(\omega)\,\mathbf{w}^T\mathbf{q}. \tag{30}$$

A modal representation of the response is introduced in the form

$$\mathbf{q} = \sum_j \mathbf{u}_j\,x_j, \quad \mathbf{u}_j^T\mathbf{M}\mathbf{u}_k = \delta_{jk}, \tag{31}$$

where $\mathbf{u}_j$ denotes the j'th mode shape vector, and x_j the corresponding modal amplitude. The second equation, where δ_{jk} denotes Kronecker's delta, normalizes the modes corresponding to unit modal mass. The following analysis concentrates on control of the first mode, and an important parameter then is

$$\nu_1 = \mathbf{w}^T\mathbf{u}_1, \tag{32}$$

representing the displacement of the mode shape vector $\mathbf{u}_1$ across the actuator.

Control of the first mode is based on the corresponding modal equation, following from (29) by pre-multiplication with the mode shape vector $\mathbf{u}_1^T$,

$$G_{qq}(\omega)\, x_1 \;+\; \nu_1 G_{q\eta}(\omega)\, \eta \;=\; F_1, \tag{33}$$

where the modal frequency response is given in terms of the undamped modal frequency ω_1 as

$$G_{qq}(\omega) \;=\; \omega_1^2 - \omega^2 \tag{34}$$

and $F_1 = \mathbf{u}_1^T \mathbf{F}$ is the corresponding external modal load.

In the control equation (30) the displacement across the actuator $\mathbf{w}^T\mathbf{q}$ contains contributions from background modes as well as the mode to be controlled. For flexible structures it is important to include the effect of these 'background modes'. A representation of this effect is obtained by constructing an approximate form of the displacement vector $\mathbf{q}$ from inversion of the homogeneous equation of motion (29),

$$\mathbf{w}^T\mathbf{q} \;=\; -\mathbf{w}^T(\mathbf{K} \,-\, \omega^2\mathbf{M})^{-1}\mathbf{w}\, G_{q\eta}(\omega)\, \eta. \tag{35}$$

The inverse of the dynamic stiffness matrix can be expanded in terms of the mode shape vectors, whereby

$$(\mathbf{K} \,-\, \omega^2\mathbf{M})^{-1} \;=\; \sum_j \frac{\mathbf{u}_j\mathbf{u}_j^T}{\omega_j^2 - \omega^2} \;\simeq\; \frac{\mathbf{u}_1\mathbf{u}_1^T}{\omega_1^2 - \omega^2} \;+\; \sum_{j=2} \frac{\mathbf{u}_j\mathbf{u}_j^T}{\omega_j^2}. \tag{36}$$

In the second, approximate form, the contributions from the higher modes have been replaced by their static counterparts. When using the full expansion at zero frequency,

$$\mathbf{K}^{-1} \;=\; \sum_j \frac{\mathbf{u}_j\mathbf{u}_j^T}{\omega_j^2}, \tag{37}$$

the summation in (36) can be eliminated, whereby

$$(\mathbf{K} \,-\, \omega^2\mathbf{M})^{-1} \;\simeq\; \frac{\mathbf{u}_1\mathbf{u}_1^T}{\omega_1^2 - \omega^2} \;+\; \Big(\mathbf{K}^{-1} - \frac{\mathbf{u}_1\mathbf{u}_1^T}{\omega_1^2}\Big). \tag{38}$$

In this form the term in the parentheses represents the effect of the higher modes.

When this representation is substituted into the expression (35) for $\mathbf{w}^T\mathbf{q}$, the following form is obtained

$$\mathbf{w}^T\mathbf{q} \;\simeq\; -\Big[\,\frac{\nu_1^2}{G_{qq}(\omega)} \;+\; \kappa_1\,\Big]\, G_{q\eta}(\omega)\, \eta \;=\; \nu_1 x_1 \;-\; \kappa_1\, G_{q\eta}(\omega)\, \eta, \tag{39}$$

where the denominator $G_{qq}(\omega)$ is the frequency function (34) of the first mode, and the modal response x_1 has been introduced from the homogeneous form of (33).

The parameter κ_1, representing the effect of the higher modes, is defined as

$$\kappa_1 \;=\; \mathbf{w}^T\Big(\mathbf{K}^{-1} - \frac{\mathbf{u}_1\mathbf{u}_1^T}{\omega_1^2}\Big)\mathbf{w} \;=\; \mathbf{w}^T\mathbf{K}^{-1}\mathbf{w} \;-\; (\nu_1/\omega_1)^2\,. \tag{40}$$

The parameter κ_1 has a direct physical interpretation. The first term is the displacement between the degrees of freedom of the sensor for a unit force exerted by the actuator, and the second term subtracts the part associated with the first mode. It is convenient to represent this parameter in the normalized form

$$\kappa \;=\; (\omega_1/\nu_1)^2\;\kappa_1 \;=\; (\omega_1/\nu_1)^2\;\mathbf{w}^T\mathbf{K}^{-1}\mathbf{w} \;-\; 1, \tag{41}$$

giving the relative extra flexibility contained in the higher modes.

The final form of the control equation for the first mode is now obtained by substituting the approximate displacement representation (39) into the control equation (30). The combined set of equations for the first mode and the controller then takes the form

$$\begin{aligned} G_{qq}(\omega)\,x_1 + \nu_1 G_{q\eta}(\omega)\,\eta &= F_1 \\ \nu_1 G_{\eta q}(\omega)\,x_1 + \big[G_{\eta\eta}(\omega) - \kappa_1 G_{\eta q}(\omega)G_{q\eta}(\omega)\big]\,\eta &= 0. \end{aligned} \tag{42}$$

It is seen that the resonator frequency function $G_{\eta\eta}(\omega)$ is modified by the term $\kappa_1 G_{\eta q}(\omega)G_{q\eta}(\omega)$, and the coupling is modified by the coefficient ν_1, representing the modal displacement across the actuator as defined in (32).

5.2 MDOF System with Acceleration Feedback

The calibration procedure consists in establishing an equivalence with the optimal control of the SDOF system presented in Sect. 4. The modal frequency function and the resonant controller are represented in the form

$$G_{qq}(\omega) \;=\; \omega_1^2 \;-\; \omega^2, \quad G_{\eta\eta}(\omega) \;=\; \omega_\eta^2 \;-\; \omega^2 \;+\; 2i\zeta_\eta\omega_\eta\omega. \tag{43}$$

In the case of acceleration feedback the sensor and actuator functions are given as

$$G_{\eta q}(\omega) \;=\; \omega^2, \quad \nu_1^2 G_{q\eta}(\omega) \;=\; \alpha_\eta\omega_\eta^2 \;+\; \beta_\eta\,2i\zeta_\eta\omega_\eta\omega. \tag{44}$$

The calibration of optimal parameters consists of finding expressions for the controller frequency ω_η and damping ratio ζ_η as well as the gain parameters α_η and β_η in terms of a common gain parameter.

The first step is the identification of the equivalent frequency and damping parameters of the controller, represented by the terms in the square brackets in (42),

$$G_{\eta\eta}(\omega) - \kappa_1 G_{\eta q}(\omega) G_{q\eta}(\omega) \\ = \omega_\eta^2 - \big[1 + \kappa\alpha_\eta(\omega_\eta/\omega_1)^2\big]\omega^2 + 2i\zeta_\eta\omega_\eta\omega\big[1 - \kappa\beta_\eta(\omega/\omega_1)^2\big]. \quad (45)$$

The last term in this expression is cubic in ω, and does not fit into the format established for the SDOF system. This term is mainly important around resonance, and thus the factor $(\omega/\omega_1)^2$ is set equal to 1 in the last square brackets. In the original SDOF format the frequency function of the controller was introduced in normalized form, and therefore the present modified frequency format is rewritten in normalized form with unit coefficient to ω^2,

$$G_{\eta\eta}(\omega) - \kappa_1\, G_{\eta q}(\omega) G_{q\eta}(\omega) = \big[1 + \alpha_\eta\kappa(\omega_\eta/\omega_1)^2\big] \\ \times\left[\frac{\omega_\eta^2}{1 + \kappa\alpha_\eta(\omega_\eta/\omega_1)^2} - \omega^2 + 2i\zeta_\eta\omega_\eta\omega\frac{1 - \kappa\beta_\eta}{1 + \kappa\alpha_\eta(\omega_\eta/\omega_1)^2}\right]. \quad (46)$$

The terms in the square brackets are now identified with the frequency function $G_{yy}(\omega)$ given in (6). This gives the two relations

$$\omega_c^2 = \frac{\omega_\eta^2}{1 + \kappa\alpha_\eta(\omega_\eta/\omega_1)^2}, \quad \zeta_c\omega_c = \zeta_\eta\omega_\eta\frac{1 - \kappa\beta_\eta}{1 + \kappa\alpha_\eta(\omega_\eta/\omega_1)^2}. \quad (47)$$

Similarly the product $G_{xy}(\omega)G_{yx}$ from the SDOF formulation (11) with $\gamma = 0$ can be identified with the off-diagonal product of the modified formulation, taking the form

$$\frac{\nu_1^2 G_{\eta q}(\omega) G_{q\eta}(\omega)}{1 + \kappa\alpha_\eta(\omega_\eta/\omega_1)^2} = \frac{\omega^2}{1 + \kappa\alpha_\eta(\omega_\eta/\omega_1)^2}\big[\alpha_\eta\omega_\eta^2 + \beta_\eta\, 2i\zeta_\eta\omega_\eta\omega\big]. \quad (48)$$

Comparison with $G_{xy}(\omega)G_{yx}(\omega)$ from (11) gives the two relations

$$\alpha\omega_c^2 = \frac{\alpha_\eta\omega_\eta^2}{1 + \kappa\alpha_\eta(\omega_\eta/\omega_1)^2}, \quad \beta\zeta_c\omega_c = \frac{\beta_\eta\zeta_\eta\omega_\eta}{1 + \kappa\alpha_\eta(\omega_\eta/\omega_1)^2}. \quad (49)$$

The four relations in (47) and (49) permit a parametric expression of the optimal MDOF gain parameters α_η, β_η and the controller frequency ω_η and the damping ratio ζ_η. It turns out to be convenient to formulate the parameter representation in terms of the equivalent SDOF gain parameter β.

The gain parameter α_η is determined by eliminating ω_c^2 between (47a) and (49a), whereby

$$\alpha_\eta = \alpha = \beta, \quad (50)$$

where the last relation follows from (23). The gain parameter β_η follows similarly by eliminating $\zeta_c\omega_c$ between (47b) and (49b),

$$\beta_\eta = \frac{\beta}{1+\kappa\beta}. \tag{51}$$

These relations imply that $\alpha_\eta > \beta_\eta$, when the effect of increased flexibility from background modes is included. The classic tuned mass damper [1, 3] can be represented by the present acceleration feedback format with $\alpha = \beta$. It follows that this relation puts limitations on the optimality of the tuning, when applied to MDOF systems with influence from background modes.

The frequency ratio of the MDOF controller ω_η/ω_1 is determined from (49a), when written in the form

$$\Big(\frac{\omega_\eta}{\omega_c}\Big)^2 = \Big(\frac{\omega_1}{\omega_c}\Big)^2\Big(\frac{\omega_\eta}{\omega_1}\Big)^2 = 1 + \kappa\beta\Big(\frac{\omega_\eta}{\omega_1}\Big)^2. \tag{52}$$

In this relation the frequency ratio $\omega_1/\omega_c = 1+\beta$ corresponds to the optimal tuning frequency ratio (21) of the SDOF system. The equation then gives the optimal MDOF frequency as

$$\omega_\eta^2 = \frac{1}{1-\dfrac{\kappa\beta}{(1+\beta)^2}}\Big(\frac{\omega_1}{1+\beta}\Big)^2. \tag{53}$$

The effect of the background modes is represented by the first factor. It vanishes for $\kappa = 0$ and leads to an increase in the tuning frequency ω_η with increasing influence of the background flexibility.

The damping ratio ζ_η is found from (49b) in the form

$$\zeta_\eta\omega_\eta = \frac{\beta}{\beta_\eta}\left[1 + \kappa\beta\Big(\frac{\omega_\eta}{\omega_1}\Big)^2\right]\zeta_c\omega_c. \tag{54}$$

This relation can be rewritten by use of the β-ratio from (51) and the frequency ratio from (53). The result of the reduction is

$$\zeta_\eta\omega_\eta = \frac{1+\kappa\beta}{1-\dfrac{\kappa\beta}{(1+\beta)^2}}\,\frac{\zeta_c\omega_1}{1+\beta}. \tag{55}$$

The damping ratio ζ_c corresponds to optimal damping of a SDOF system and is given by (25). Also in this case the effect of the background modes is represented by the first factor.

6 Damping of Wind Excited Building

The efficiency and characteristics of the filtered acceleration feedback approach are illustrated in terms of the wind-excited benchmark building introduced in [9]. The height of the building is 306.1 m and it has 76 stories. The structure is modelled by 76 simple 2D beam elements, where the rotational degrees-of-freedom have been eliminated by static condensation. This leaves 76 degrees-of-freedom representing the horizontal displacement of each floor, see [9] for further details on the model. The time domain equations of motion for the structure with resonant control can be written in the compact form

$$\mathbf{M}_*\ddot{\mathbf{z}}(t) + \mathbf{C}_*\dot{\mathbf{z}}(t) + \mathbf{K}_*\mathbf{z}(t) = \mathbf{F}_*(t), \tag{56}$$

where the augmented vector $\mathbf{z} = [\mathbf{q}^T, \eta]^T$ contains the structural degrees-of-freedom and the control variable. The system matrices follow directly as

$$\mathbf{M}_* = \begin{bmatrix} \mathbf{M} & \mathbf{0} \\ -\mathbf{w}^T & 1 \end{bmatrix}, \qquad \mathbf{C}_* = \begin{bmatrix} \mathbf{C} & (\beta_\eta/\nu_1^2)2\zeta_\eta\omega_\eta\mathbf{w} \\ \mathbf{0}^T & 2\zeta_\eta\omega_\eta \end{bmatrix}$$
$$\mathbf{K}_* = \begin{bmatrix} \mathbf{K} & (\alpha_\eta/\nu_1^2)\omega_\eta^2\mathbf{w} \\ \mathbf{0}^T & \omega_\eta^2 \end{bmatrix}, \quad \mathbf{F}_* = \begin{bmatrix} \mathbf{F}_w \\ 0 \end{bmatrix}, \tag{57}$$

where the external force vector $\mathbf{F}_w$ represents the wind loading and $\mathbf{0}$ is a 76×1 zero column vector. The actuator force, included in the last column of $\mathbf{C}_*$ and $\mathbf{K}_*$, follows from the last term in (29) which can be computed via the control variable as

$$F_c(t) = \frac{\alpha_\eta}{\nu_1^2}\,\omega_\eta^2\eta(t) + \frac{\beta_\eta}{\nu_1^2}\,2\zeta_\eta\omega_\eta\dot{\eta}(t). \tag{58}$$

Thus, the uncontrolled case is recovered for $\alpha_\eta = \beta_\eta = 0$.

6.1 Design of Resonant Control

The mode shapes $\mathbf{u}_j$ and natural frequencies ω_j of the undamped structure are shown in Fig. 6 for the first three modes. In the following the first mode is considered as the target mode for the resonant control. A force actuator is used to apply the desired resonant control. To demonstrate the influence of the background modes two locations of the force actuator are considered, as shown in Fig. 7. The largest relative displacement of mode 1 occurs between the top floors, and this actuator location is in the following referred to as case (a). The smallest relative displacement occurs between the two bottom floors, which is case (b). In both cases the actuator is placed in a Chevron brace so that the relative motion over the actuator is equal to the relative motion between the adjacent floors. Hereby, the connectivity vectors

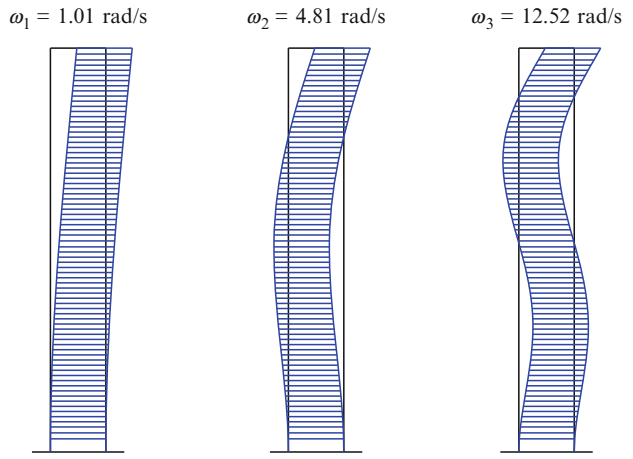

Fig. 6 Undamped mode shapes and natural frequencies for first three modes

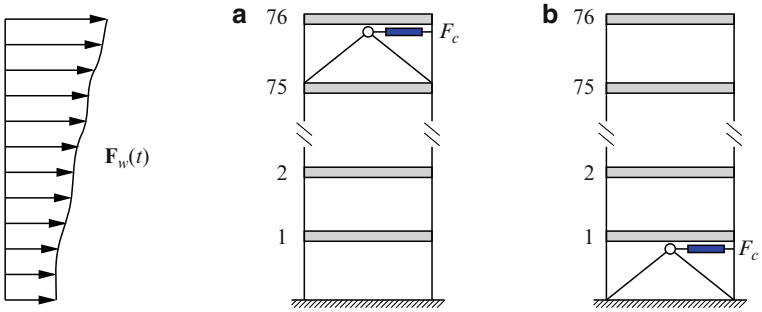

Fig. 7 76-story building with a force actuator in a Chevron brace acting between (**a**) top and (**b**) bottom floors

for case (a) and (b) are $\mathbf{w} = [0, \ldots -1, 1]^T$ and $\mathbf{w} = [1, 0, \ldots, 0]^T$, respectively. For mode 1 the non-dimensional flexibility factor is $\kappa = 1.2125$ for case (a). For case (b) it is $\kappa = 10.371$ and thereby almost an order of magnitude larger than for case (a).

The sequential design procedure is described via the first eight columns of Table 2, where the desired modal damping ratio ζ_{des} of the target mode acts as the initial design variable. In the table four design situations with $\zeta_{des} = 0.04, 0.06, 0.08$ and 0.10 are presented. Because of the equal split of modal damping it follows from (28) that the damping parameter of the resonant control should be twice the desired damping ratio: $\zeta_c = 2\zeta_{des}$. Hereafter, the gain parameter β can be found by (25). The gain parameter can also be expressed directly in terms of the desired modal damping ratio as

$$\beta = \frac{8\zeta_{des}^2}{1 - 8\zeta_{des}^2}. \tag{59}$$

Table 2 Mode 1 damping ratios for 76-story building with resonant force actuator

ζ_{des}	ζ_c	β	ω_c/ω_1	β_η	α_η	ω_η/ω_1	ζ_η	$\zeta_1^{\mp}$	$\zeta_1^{\mp}\|_{\kappa=0}$
Actuator between top floors: $\kappa = 1.2125$									
0.04	0.08	0.0130	0.9872	0.0128	0.0130	0.9949	0.0819	0.0403 0.0401	0.0429 0.0357
0.06	0.12	0.0297	0.9712	0.0286	0.0297	0.9881	0.1265	0.0610 0.0606	0.0648 0.0507
0.08	0.16	0.0540	0.9488	0.0506	0.0540	0.9780	0.1757	0.0826 0.0819	0.0858 0.0643
0.10	0.20	0.0870	0.9200	0.0787	0.0870	0.9640	0.2317	0.1058 0.1046	0.1052 0.0771
Actuator between bottom floors: $\kappa = 10.371$									
0.04	0.08	0.0130	0.9872	0.0114	0.0130	1.0590	0.0974	0.0405 0.0402	0.0505 0.0164
0.06	0.12	0.0297	0.9712	0.0227	0.0297	1.1527	0.1862	0.0620 0.0612	0.0657 0.0170
0.08	0.16	0.0540	0.9488	0.0346	0.0540	1.3469	0.3543	0.0852 0.0843	0.0717 0.0164
0.10	0.20	0.0870	0.9200	0.0457	0.0870	1.8909	0.7818	0.1078 0.1086	0.0716 0.0153

The rest of the design parameters are expressed in terms of β. The frequency of the resonant filter in the single-degree-of-freedom case follows from Table 1 as $\omega_c = \omega_1/(1+\beta)$, and finally the parameters α_η, β_η, ω_η and ζ_η for the multi-degree-of-freedom system are determined from (50), (51), (53) and (55), respectively.

6.2 Root Locus Analysis

The free vibration properties are illustrated in terms of a root locus analysis, where the complex valued natural frequencies ω are plotted in the complex plane for increasing gain β. The natural frequency is obtained by solving the corresponding eigenvalue problem that follows from the frequency domain representation of the equation of motion in (56) when both the external loading $\mathbf{F}$ and the structural damping $\mathbf{C}$ are omitted. Figure 8 shows the root loci for the two modes associated with the first vibration form of the structure. The solid curve represents the trajectories of the two natural frequencies of mode 1 when including the background flexibility, while the dashed curves represent the case without quasi-static correction. The markers represent the complex natural frequencies for the four cases in Table 2: $\zeta_{des} = 0.04, 0.06, 0.08$ and 0.1.

Figure 8a shows the root locus diagram when the actuator is operating between the top floors and it is observed that the solid curves follow the 45° trajectories similar to the ideal case in Fig. 3b. The actual modal damping ratios are given in the last two columns in Table 2. It is seen that for $\kappa = 1.2125$ the two damping ratios

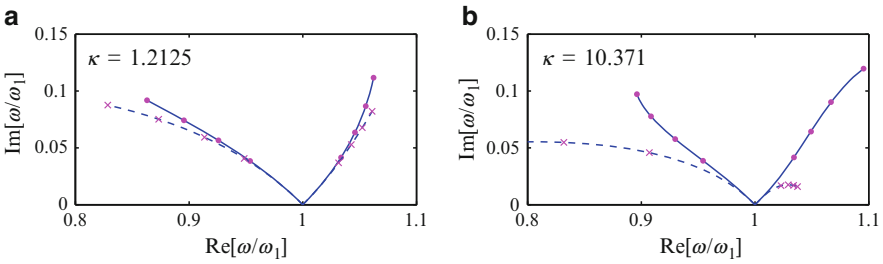

Fig. 8 Root locus diagram for mode 1. (**a**) Force actuator between top floors and (**b**) between bottom floors

are practically identical and equal to the desired value $\zeta_{des} = 0.04, 0.06, 0.08$ and 0.1. In the case without quasi-static correction for higher modes ($\kappa = 0$) the optimal equal split property is not attained, resulting in a reduced damping efficiency of the control. This effect can also be seen for the dashed loci in Fig. 8a, where the right trajectory develops too little damping.

Figure 8b shows the root locus diagram when the actuator is attached between the bottom floors. The large flexibility parameter $\kappa = 10.371$ implies that the solid trajectories in the figure deviate slightly from the ideal curves for large damping ratios. However, as seen in Table 2 the two damping ratios are still equal, although slightly larger than the desired values. In this case the importance of the quasi-static correction becomes clear when comparing to $\kappa = 0$. In that case the left dashed locus in Fig. 8b is very large while the right is very small. As seen from the last column of Table 2 the balance between the two damping ratios is completely lost in this case. Thus, when the actuator is located where the relative modal deformation is small, the κ-value becomes relatively large and the associated correction for background modes is critically important.

6.2.1 Response Analysis

The root locus analysis describes the behavior of the modal damping properties, where robust design relies on equal modal damping, which defines the filter frequency ω_c as shown in Sect. 4. However, the remaining control parameters α and ζ_c are determined to secure optimal frequency response characteristics, as shown in Fig. 4. The efficiency of the resonant control strategy for harmonic excitation of multi-degree-of-freedom structures has been demonstrated in [4], and the present example therefore verifies the performance of the resonant control strategy for random loading, in this case represented by wind excitation. The time history of the wind load is presented in [9] and has been obtained by wind tunnel tests. The wind load on the top floor is shown in Fig. 9.

The time domain equation of motion (56) is solved by the standard (average acceleration) Newmark time integration procedure, see e.g. [10]. The time increment

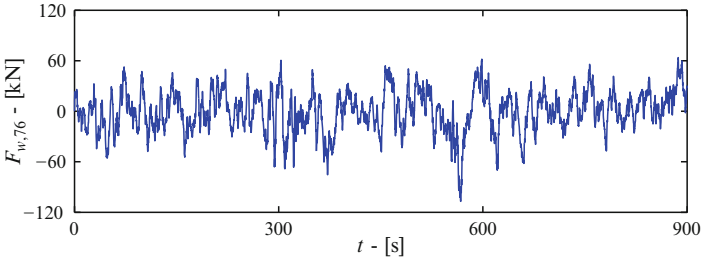

Fig. 9 Wind load history for top floor

$\Delta t = 0.1333\,\mathrm{s}$ is dictated by the sampling frequency of the wind data and corresponds to approximately 47 time increments per mode 1 vibration period of the structure. Structural damping is contained in $\mathbf{C}$ and yields 1% of critical damping in the first five modes, see [9].

In [9] a total of 12 performance criteria are presented, describing the root mean square (rms) and the peak values of the response of both the structure and the control force. Only some of these criteria are used in the present example. The maximum rms values of the structural response are evaluated in terms of the top floor response

$$J_1 = \sigma_{\ddot{q},75}/\sigma^0_{\ddot{q},75}, \quad J_2 = \sigma_{q,76}/\sigma^0_{q,76}, \tag{60}$$

where $\sigma_{q,j}$ and $\sigma_{\ddot{q},j}$ are the rms displacement and acceleration of the j'th floor, while superscript 0 refers to the case without control. Note that the acceleration criterion is based on floor 75, since floor 76 is the roof and therefore unoccupied. The third performance criterion describes the power consumption of the actuator and is determined by the time integral

$$J_3 = \sqrt{\frac{1}{T}\int_0^T \left(\dot{x}(t)F_c(t)\right)^2 dt}\,, \quad [J_3] = \mathrm{kN\,m/s}, \tag{61}$$

where $\dot{x} = \mathbf{w}^T\dot{\mathbf{q}}$ is the velocity of the actuator and $T = 900\,\mathrm{s}$ is the total length of the simulation. The integral is computed by the trapezoidal rule.

The peak response of the structure is described by

$$J_4 = \ddot{q}_{p,75}/\ddot{q}^0_{p,75}, \quad J_5 = q_{p,76}/q^0_{p,76}, \tag{62}$$

where $\ddot{q}_{p,j}$ and $q_{p,j}$ are the peak acceleration and displacement of the j'th floor. The peak power consumption of the actuator is finally defined as

$$J_6 = \max\left|\dot{x}(t)F_c(t)\right|, \quad [J_6] = \mathrm{kN\,m/s}, \tag{63}$$

where $|\cdot|$ denotes the absolute value.

Table 3 Performance criteria for resonant controller

ζ_{des}	J_1	J_2	J_3	J_4	J_5	J_6
Actuator between top floors: $\kappa = 1.2125$						
0.04	0.468	0.601	7.029	0.474	0.709	43.096
0.06	0.391	0.557	7.729	0.422	0.695	44.184
0.08	0.341	0.533	8.287	0.416	0.668	54.342
0.10	0.304	0.520	8.737	0.397	0.648	69.063
Actuator between bottom floors: $\kappa = 10.371$						
0.04	0.464	0.598	7.912	0.461	0.707	46.543
0.06	0.389	0.553	9.402	0.412	0.694	52.036
0.08	0.344	0.529	11.108	0.409	0.679	63.216
0.10	0.318	0.514	13.081	0.398	0.668	96.043
Sample controller [9]						
	0.369	0.578	11.99	0.381	0.717	71.96

The six performance criteria are summarized in Table 3 for the two actuator locations and the four desired damping ratios also used in the root locus analysis. The bottom row in the table gives the corresponding performance criteria for the LQG sample controller in the benchmark paper [9]. It is seen that the structural rms values J_1 and J_2 are reduced with increasing desired damping and good performance is observed compared to the LQG reference case in [9]. It should be noted that the reduction in structural response is practically the same for the two actuator locations. In general it is observed that the influence of κ is mainly on the power needed to realize the required actuator force, in the Table represented by J_3 and J_6. It is also noted that the reduction in the peak values is not as significant as for the rms values. This is because the resonant controller is designed with respect to stationary response, whereby the ability to reduce peak response from transients, such as wind gusts and earthquakes, is limited.

7 Conclusions

A design principle for resonant control of a SDOF system by second order filters has been presented. It covers the two cases of modified acceleration feedback and modified displacement feedback and includes the classic tuned mass damper as a special case of acceleration feedback. A set of explicit formulae is obtained for the optimal control parameters by combining the root locus property of equal modal damping with optimal response curve characteristics.

The procedure is extended to collocated resonant control of the lower modes of MDOF systems. In this case the response recorded by the sensor typically includes contributions from the motion of higher modes. An explicit design procedure for the control parameters of MDOF systems has been developed that includes the effect of the higher modes via a quasi-static approximation. A numerical example

in the form of a benchmark problem involving turbulent wind load on a high-rise building illustrates the potential of resonant control, and demonstrates the importance of including a quasi-static correction of the control parameters, in particular when the control force is applied close to the supports of the structure.

References

1. Den Hartog, J.P.: Mechanical Vibrations, 4th edn. McGraw-Hill, New York (1956)
2. Preumont, A.: Vibration Control of Active Structures. An Introduction, 2nd edn. Kluwer, Dordrecht (2002)
3. Krenk, S.: Frequency analysis of the tuned mass damper J. Appl. Mech. ASME **72**, 936–942 (2005)
4. Krenk, S., Høgsberg, J.: Optimal resonant control of flexible structures J. Sound Vib. **323**, 530–554 (2009)
5. Ozer, M.B., Royston, T.J.: Application of Sherman-Morrison matrix inversion formula to damped vibration absorbers attached to multi-degree of freedom systems. J. Sound Vib. **283**, 1235–1249 (2005)
6. Ozer, M.B., Royston, T.J.: Extending Den Hartog's vibration absorber technique to multi-degree of freedom systems. J. Vib. Acoust. **127**, 341–350 (2005)
7. Krenk, S., Høgsberg, J.: Tuned mass absorbers on damped structures under random load. Probabilistic Eng. Mech. **23**, 408–415 (2008)
8. Hansteen, O.E., Bell, K.: Accuracy of mode superposition analysis in structural dynamics. Earthquake Eng. Struct. Dyn. **7**, 405–411 (1979)
9. Yang, J.N., Agrawal, A.K., Samali, B., Wu, J-.C.: Benchmark problem for response control of wind-excited tall buildings. J. Eng. Mech. **130**, 437–446 (2008)
10. Geradin, M., Rixen, D.: Mechanical Vibrations, 2nd edn. Wiley, Chichester (1997)

http://www.springer.com/978-90-481-9986-0

Computational Methods in Stochastic Dynamics
Papadrakakis, M.; Stefanou, G.; Papadopoulos, V. (Eds.)
2011, XII, 342 p., Hardcover
ISBN: 978-90-481-9986-0